

## Bimetallic nanopetals for thousand-fold fluorescence enhancements

Chi-Cheng Fu,<sup>1</sup> Giulia Ossato,<sup>2</sup> Maureen Long,<sup>3</sup> Michelle A. Digman,<sup>2,4</sup> Ajay Gopinathan,<sup>5</sup> Luke P. Lee,<sup>1</sup> Enrico Gratton,<sup>2</sup> and Michelle Khine<sup>2,a)</sup>

<sup>1</sup>Department of Bioengineering, University of California, Berkeley, 94720 California, USA

<sup>2</sup>Department of Biomedical Engineering, University of California, Irvine, 92697 California, USA

<sup>3</sup>School of Engineering, University of California, Merced, 95344 California, USA

<sup>4</sup>Development Biology Center, University of California, Irvine, 92697 California, USA

<sup>5</sup>School of Natural Sciences, University of California, Merced, 95344 California, USA

(Received 12 July 2010; accepted 3 September 2010; published online 15 November 2010)

We present a simple, ultra-rapid and robust method to create sharp nanostructures—nanopetals—in a shape memory polymer substrate demonstrating unprecedented enhancements for surface enhanced sensing over large surface areas. These bimetallic nanostructures demonstrate extremely strong surface plasmon resonance effects due to the high density multifaceted petal structures that increase the probability of forming nanogaps. We demonstrate that our nanopetals exhibit extremely strong surface plasmons, confining the emission and enhancing the fluorescence intensity of the nearby high-quantum yield fluorescein by  $>4000\times$ . The enhancements are confined to the extremely small volumes at the nanopetal borders. This enables us to achieve single molecule detection at relatively high and physiological concentrations. © 2010 American Institute of Physics. [doi:10.1063/1.3495773]

Nanoplasmonic methods utilizing metallic nanostructures that interact with fluorescent species to enhance their signals and to confine their detection volumes have been developed.<sup>1</sup> Zero-mode waveguides (ZMW),<sup>2</sup> metallic nanoparticles,<sup>3</sup> metal tips,<sup>4</sup> nanopockets,<sup>5</sup> optical antennas,<sup>6</sup> and feed gaps<sup>7</sup> have achieved atto-to zeptoliter excitation volumes and 1-to 1,000-times enhancements of fluorescence emission. Recently, bowtie nanoantennas to facilitate detection of single molecules showed a 1,340-fold increase in fluorescence intensity of the low fluorescence quantum efficiency dye (TPQDI).<sup>8</sup> However, these nanoplasmonic structures are produced by expensive and sophisticated nanofabrication techniques.<sup>1</sup> Lowering the fabrication threshold and developing microfluidic integratable metallic nanostructures would widen their applicability and accessibility for biomedical applications.<sup>9</sup>

We recently presented a simple, ultra-rapid low-cost method to create large scale metallic nanowrinkles on polystyrene (PS) sheets.<sup>9</sup> These tunable wrinkles can be easily integrated into microchannels.<sup>9–12</sup> In applying them for fluorescence enhancement, though, the intensity of their hotspots were hampered by their smoothness and continuousness that cannot localize and concentrate electromagnetic field as well as sharp and discrete ones.<sup>1</sup> Here, we present sharp nanostructures, coined nanopetals, to overcome this limitation. These bimetallic petals (comprised of gold coated silver) with nanosawtoothlike edges show strong surface plasmon resonance (SPR) effects. High-density multifaceted petal structures increase the probability of forming nanogaps, which can improve enhancements by approximately one thousand times, compared with continuous metal strips.<sup>1,7</sup>

In Fig. 1(a), a 80 nm thick Ag film followed by a 80 nm thick Au film is deposited on a prestressed PS sheet (KSF50-C; Grafix,  $2\times 1\text{ cm}^2$ ) using a sputter coater (Polaron coating system).<sup>9</sup> Subsequent heating at 160 °C (above

PS glass transition temperature) for 6 min induces retraction of the substrate and causes the nonshrinkable metallic films to wrinkle and crack. Cracking is critical to create these nanosawtooth structures on the edges of the petals, while buckling improves the formation of nanogaps. Scanning electron micrographs (SEM) confirm large areas of biaxial nanogaps [Fig. 1(b)]. Uniaxial petals can be created as well [Fig. 1(c)] by clamping two edges of a metal-coated sheet with binder clips (2" binder clips; OfficeMax) during heating for retraction only in one direction.

Nanofeatures, including the shape of the nanostructures and the dimension of the resulting gaps between them, deter-

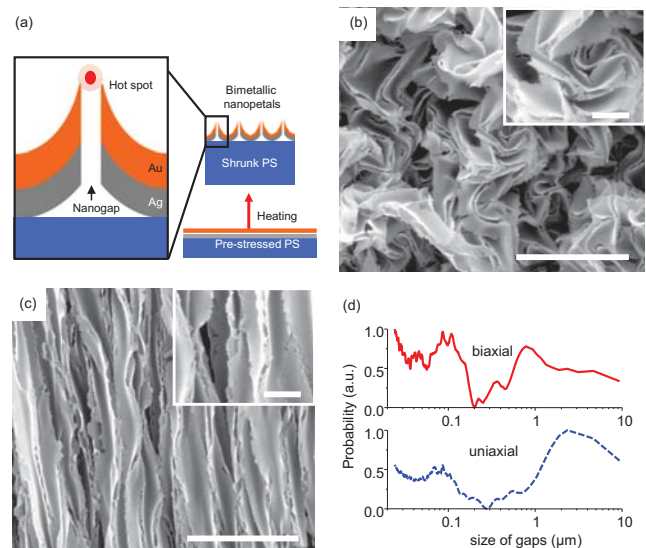


FIG. 1. (Color online) (a) Schematic of fabrication process and creation of hot spots on bimetallic nanopetals. SEM images with large-scale biaxial (b) and uniaxial (c) Au/Ag petals on shrunken PS sheets. The insets in (b) and (c) show corresponding enlarged view of SEM images. The scale bars in (b) and (c) are 10  $\mu\text{m}$ . The scale bars in inset of (b) and (c) are 2  $\mu\text{m}$ . (d) Histograms of gaps dimensions are normalized by their maximum values.

<sup>a)</sup>Electronic mail: mkhine@uci.edu.

mine the density and intensity of hotspots.<sup>1</sup> SEMs show that cracking creates very sharp sawtoothlike edges [insets of Figs. 1(b) and 1(c)]. The sizes of these saw-teeth are smaller than 100 nm. Because buckling is involved in fabrication, these petals are highly folded and compressed, which improves nanogap formation. To determine the dimension of these nanogaps, an edge detection program (the Canny method, MATLAB<sup>®</sup> software) was applied to the SEM followed by two-dimensional fast Fourier transform (2D FFT).<sup>9</sup> Distribution of gap dimensions [Fig. 1(d)] is obtained by further transforming corresponding power spectral densities to real space. Both bi- and uniaxial samples exhibit two discrete populations. The large one, ranging from 200 nm to 10  $\mu\text{m}$ , is attributed to the wrinkling process;<sup>9</sup> the small one, ranging from 20 to 200 nm, reflects the dimension of the nanogaps of interest. Such tiny gaps, along with nanoscale shapes, render nanopetals an extremely effective substrate for metal-enhanced fluorescence techniques.

To localize and measurement hotspots, fluorescein molecules are dissolved in water (pH=9.0, concentration 1  $\mu\text{M}$ ). 50  $\mu\text{L}$  dye solution is dropped onto the biaxial and uniaxial petals. Samples are covered by a glass coverslip (no.1.5) and mounted on a Zeiss LSM 710 microscopy with 3D scanning systems.<sup>4</sup> The microscope is coupled to a mode-locked two-photon Ti-sapphire laser (0.3 mW, Spectra-Physics, Mountain View, CA) operated at 790 nm with a 80-MHz repetition rate. Samples are excited with a 40 $\times$  objective (C-Apochromat 40 $\times$ /1.20NA Water Corr, Carl Zeiss, Jena, Germany), and emitted fluorescence light are selected by a spectral detector between 513–593 nm and detected with a photo multiplier tube. Figure 2(a) shows that bright fluorescence emission can be observed on the petals, and more importantly, extremely bright spots can be found at the edges of the petals. Their vertical cross-section images [Fig. 2(b)] show that the fluorescence intensity from the edges are about 100-fold higher than that from background. That indicates the enhancement attributes to strong plasmonic interactions between dye molecules and hotspots on the edge of petals [Fig. 1(a)].

The hotspot volume is estimated by the diffusion of fluorescein through the volume of excitation using amplitude analysis (similar to the photon counting histogram method).<sup>13</sup> The laser focusing spot with 1.8 mW laser power is fixed on the edges of petals, and time trace of fluorescence intensity is recorded [Fig. 2(c)]. The curves show bursts of intensity when a fluorescein molecule diffuses into a hotspot; after that the intensity dramatically drops to background.<sup>2,8</sup> The width of each burst is only  $\approx 2 \mu\text{s}$  (inset) which indicates the extremely tiny enhancement region. Comparing the number of very large bursts with the number of bursts expected from a solution 1  $\mu\text{M}$  fluorescein in the 2P confocal excitation volume ( $10^{-15}$  L) we estimate that less than 1/1000 of the molecules are enhanced. Based on these results, we estimate that an upper limit of the volume in which we have enhancement (the size of hot spots) is about  $10^{-18}$  L, similar to that of ZMW.<sup>2</sup>

Figure 3(a) left shows that increasing the laser power increases the population of hot spots and their enhanced fluorescence intensities. With average laser power higher than 1.8 mW, we observe thousands-folds enhancements that saturate our detector [larger than 4,095 counts, green arrows in the Fig. 3(a), left]. Note that the intensity from molecules

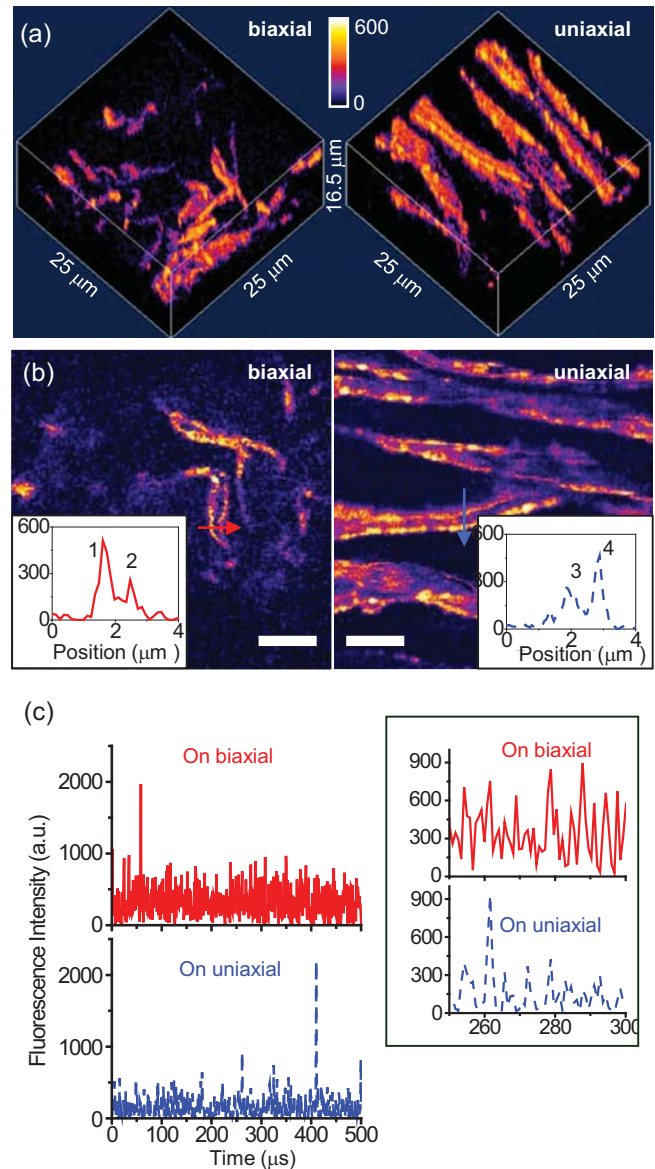


FIG. 2. (Color online) (a) Three-dimensional two photon excitation fluorescence images of fluorescein molecules on biaxial (left) and uniaxial (right) nanopetals. (b) Vertical cross-section images and the intensity profiles (insets) along the arrows. The FWHMs of enhancement regions (denoted by “1” to “4”) are diffraction-limited size ( $\approx 300$  nm). The scale bars are 5  $\mu\text{m}$ . (c) Time traces of fluorescence emission from molecules enhanced on the edges of biaxial petals (solid line) and uniaxial (dashed line) petals, along with their enlarged views (inset).

without enhancement is between 1 to 5 counts. This becomes even more obvious at higher excitation power (3 mW) as shown in Fig. 3(a), right. In SPR the fluorescence enhancement is accompanied by a decrease in the fluorescence lifetime.<sup>3</sup> The intensity decays are measured on a home built 2P laser scanning microscope equipped with a similar Mai Tai laser and an objective as mentioned above. All lifetime data are collected with time correlated single-photon counting card (SP830 B&H, Becker & Hickl GmbH, Berlin, Germany). Figure 3(b) shows average fluorescence excitation state lifetime of fluorescein in solution is  $\approx 3.7$  ns. In the region around the nanopetals, the lifetime decreases to less than 100 ps, below the detection limit of our system. This indicates greater than 37-fold reduction in fluorescence lifetime and further confirms that the fluorescence enhancement is due to SPR. Overall, these results indicate that our nano-

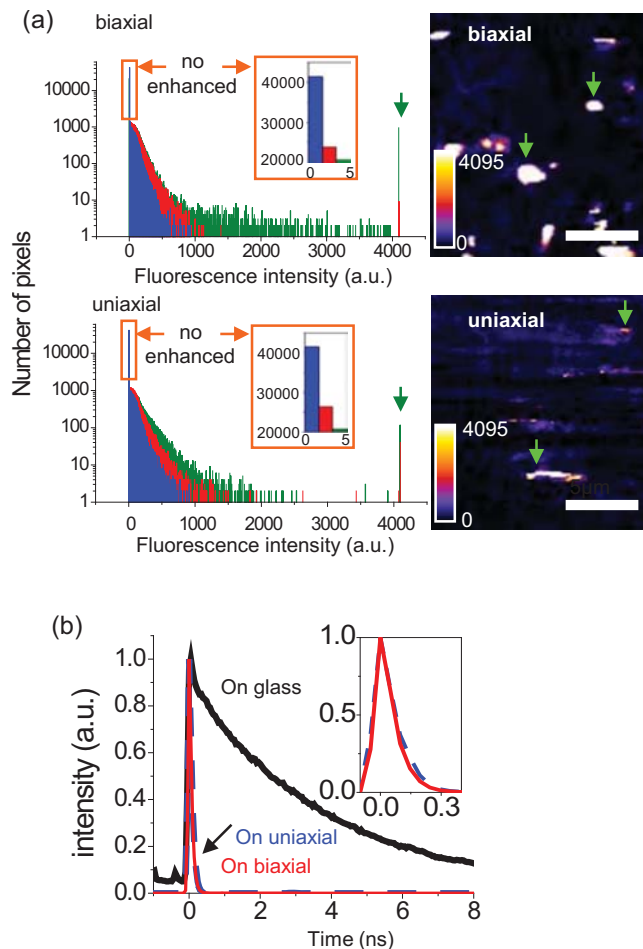


FIG. 3. (Color online) (a) Left: fluorescence intensity histograms of dye molecules on biaxial (top) and uniaxial (bottom) nanopetals excited by various laser powers (blue: 0.6 mW, red: 1.8 mW, green: 3 mW). Right: at 3 mW excitation power, corresponding fluorescence images show many spots emitting bright fluorescence which saturate the avalanche photodiode. Green arrows indicate the saturation point. (b) Fluorescence lifetime measurements of dyes on a glass plate (top line), biaxial petals (solid line), and uniaxial petals (dashed line).

petals exhibit extremely strong surface plasmons, confining the emission and enhancing the fluorescence intensity of the nearby high-quantum yield fluorophore, fluorescein, by several thousand-folds, which is significantly greater than previous reports.<sup>14,15</sup> Note that high quantum yield dyes are notoriously more difficult to enhance as compared to low quantum yield ones.<sup>8</sup>

Besides the strong SPR effects, Au/Ag alloy nanostructures hold a number of advantages over a single pure metal, including easier surface functionalization, better plasmon tunability and broader surface plasmon band for multiple-probe enhancement.<sup>16</sup> Our method can be easily integrated with microfluidic devices to combine with high throughput

lab-on-chip techniques.<sup>9–12,17</sup> Importantly, because of–not in spite of–the “variability” in our substrate, we do not need to choose an esoteric dye such that it would match our plasmon resonance. Because we have a range of nanostructure and nanogap sizes, we can ensure that we can achieve huge fluorescence enhancements on our substrate. These advantages show great potential for low-cost biomedical sensing at single molecular levels at physiological concentrations.<sup>2,4,8</sup> Finally, the extremely confined and strong hot spots of the nanopetals can be used as substrates for studying highly localized events on cell membranes and for direct detection of cell secretion molecules without further amplification.<sup>3</sup>

Authors Fu & Ossato contributed equally to this work. Supported by NIH-P41 under Grant No. P41-RRO3155 (E.G. and G.O.), under Grant No. U54 GM064346 Cell Migration Consortium (M.D. and E.G.), UC Cancer Support under Grant No. CA-62203 (M.D.) through the Developmental Biology Center’s Biology Optical Core Facility, and Shrink Nanotechnologies Inc. The author Khine is the scientific founder of Shrink but receives no compensation nor does she have any financial interest in the company. Terms of this arrangement have been reviewed and approved by UC Irvine in accordance with its conflict of interest policies.

- <sup>1</sup>S. Kawata, Y. Inouye, and P. Verma, *Nat. Photonics* **3**, 388 (2009).
- <sup>2</sup>M. J. Levene, J. Korlach, S. W. Turner, M. Foquet, H. G. Craighead, and W. W. Webb, *Science* **299**, 682 (2003).
- <sup>3</sup>J. Zhang, Y. Fu, D. Liang, K. Nowaczyk, R. Y. Zhao, and J. R. Lakowicz, *Nano Lett.* **8**, 1179 (2008).
- <sup>4</sup>E. J. Sánchez, L. Novotny, and X. S. Xie, *Phys. Rev. Lett.* **82**, 4014 (1999).
- <sup>5</sup>G. L. Liu, J. Kim, Y. Lu, and L. P. Lee, *Appl. Phys. Lett.* **89**, 241118 (2006).
- <sup>6</sup>M. F. Garcia-Parajo, *Nat. Photonics* **2**, 201 (2008).
- <sup>7</sup>P. Muhlshlegel, H. J. Eisler, O. J. Martin, B. Hecht, and D. W. Pohl, *Science* **308**, 1607 (2005).
- <sup>8</sup>A. Kinkhabwala, Z. Yu, S. Fan, Y. Avlasevich, K. Müllen, and W. E. Moerner, *Nat. Photonics* **3**, 654 (2009).
- <sup>9</sup>C. C. Fu, A. Grimes, M. Long, C. G. L. Ferri, B. D. Rich, S. Ghosh, S. Ghosh, L. P. Lee, A. Gopinathan, and M. Khine, *Adv. Mater.* **21**, 4472 (2009).
- <sup>10</sup>A. Grimes, D. N. Breslauer, M. Long, J. Pegan, L. P. Lee, and M. Khine, *Lab Chip* **8**, 170 (2008).
- <sup>11</sup>C. S. Chen, D. N. Breslauer, J. I. Luna, A. Grimes, W. C. Chin, L. P. Leeb, and M. Khine, *Lab Chip* **8**, 622 (2008).
- <sup>12</sup>M. Long, M. A. Sprague, A. A. Grimes, B. D. Rich, and M. Khine, *Appl. Phys. Lett.* **94**, 133501 (2009).
- <sup>13</sup>Y. Chen, J. D. Muller, P. T. So, and E. Gratton, *Biophys. J.* **77**, 553 (1999).
- <sup>14</sup>H. Szmazinski and J. R. Lakowicz, *Anal. Chem.* **80**, 6260 (2008).
- <sup>15</sup>S. A. Patel, C. I. Richards, J. C. Hsiang, and R. M. Dickson, *J. Am. Chem. Soc.* **130**, 11602 (2008).
- <sup>16</sup>H. Yoo, J. E. Millstone, S. Li, J. W. Jang, W. Wei, J. Wu, G. C. Schatz, and C. A. Mirkin, *Nano Lett.* **9**, 3038 (2009).
- <sup>17</sup>P. C. Hidber, P. F. Nealey, W. Helbig, and G. M. Whitesides, *Langmuir* **12**, 5209 (1996).